Article

Not peer-reviewed version

Decentralized Thermochemical Conversion of Local Biomasses: Energy Recovery and Biochar Production in Resource-Limited Arid Regions

Karim Zongo *, Moussa dit Corneille Tarpilga, Yssa Traoré, Bétaboalé Naon, Hervé Pierre Ravelonandro

Posted Date: 27 February 2026

doi: 10.20944/preprints202602.1526.v1

Keywords: slow pyrolysis; waste valorization; biochar; energy

 doi:10.20944/preprints202602.1526.v1

Article

Decentralized Thermochemical Conversion of Local Biomasses: Energy Recovery and Biochar Production in Resource-Limited Arid Regions

Karim Zongo [1,2,*], Moussa dit Corneille Tarpilga [3], Yssa Traoré [1], Bétaboalé Naon [1] and Hervé Pierre Ravelonandro [2]

[1] Laboratory of Materials, Heliophysics and Environment (La.M.H.E), Nazi Boni University, Bobo-Dioulasso, Burkina Faso

[2] Research Unit in Process Engineering and Environmental Engineering, University of Antananarivo, Antananarivo, Madagascar

[3] Materials and Environment Laboratory (LAME), Joseph Ki-Zerbo University, Ouagadougou, Burkina Faso

* Correspondence: zongkarimtita@gmail.com

Abstract

The valorization of underexploited biomass in arid regions represents an important pathway for decentralized energy production and sustainable soil management. Although biomass pyrolysis has been widely investigated, most studies are conducted under controlled laboratory conditions, with limited assessment of low-technology systems operating under real domestic use. This study evaluates the thermochemical behavior and energy performance of locally available biomasses using a multifunctional household oven. Millet stalks, cashew nut shells, cashew nut shell cake, and rumen contents were subjected to slow pyrolysis. Temperature evolution in the pyrolysis and combustion chambers was continuously monitored using type 'K' thermocouples, and mass and energy balances were applied to assess product distribution and process efficiency. Pyrolysis temperatures ranged between approximately 270 and 350 °C, while combustion temperatures reached up to 800 °C depending on the biomass. Product yields varied significantly according to feedstock characteristics. Cashew nut shells showed the highest energy efficiency (about 71%), followed closely by millet stalks, whereas rumen contents presented lower performance. Thermal profiles consistently revealed four successive phases governed by biomass composition and reactor–biomass interaction. These findings confirm the technical feasibility of household-scale pyrolysis for combined energy recovery and biochar production under realistic operating conditions.

Keywords: slow pyrolysis; waste valorization; biochar; energy

1. Introduction

The valorization of residual biomass represents a major challenge for sustainable development (Laurent et al., 2011). This is part of a broader context of energy transition, waste management, sustainable agriculture, and climate change mitigation (Laird, 2008). Drought, deforestation, soil depletion, and energy shortages are widespread problems in most parts of the world, but they are particularly acute in arid regions such as Burkina Faso. The excessive use of chemical fertilizers to improve crop yields depletes the soil, reducing organic matter content and fertility. This, in turn, leads to further degradation of agricultural soil quality, environmental pollution, and a decrease in essential nutrients, thus threatening the ecosystem (Siddiqui et al., 2019). It is therefore crucial to explore alternatives to chemical fertilizers that are available in large quantities, promote food production, improve CO_2 sequestration, and preserve soil health and the environment (C.F.D.T & agro-alimentaire, 1981). In this case, biomass valorization presents itself as a promising alternative or supplement. (Paudel et al., 2024). Biomass valorization processes are currently being developed in

 doi:10.20944/preprints202602.1526.v1

various ways, including thermochemical processes (Chormare et al., 2023). Among the thermochemical processes used to transform biomass into high value-added products, pyrolysis stands out as a promising technique. It converts organic matter into three main fractions: a combustible gas, a liquid rich in organic compounds, and a solid carbonaceous residue called biochar. (Lewandowski et al., 2020). Nowadays, the energy and agricultural applications of biochar are attracting increasing interest (Armah et al., 2022; Graça et al., 2024). Biochar technology has seen significant advancements, particularly in recent years. More in-depth studies are being conducted in laboratories, and field applications are rapidly developing in locations such as the Northern countries, China, and elsewhere. However, in Southern countries, particularly in the Sahel region such as Burkina Faso, biochar technology is still in its infancy. These regions face energy and agricultural challenges exacerbated by climate change. These difficult situations are particularly acute in rural areas, where insecurity also creates problems of access to resources and arable land. In this context, the valorization of biomass, including organic residues from the agri-food and agricultural industries, is emerging as a potential solution to address these interconnected challenges. Millet stalks, cashew nut shells, and organic waste from slaughterhouses are locally available biomass resources that, until now, have often been underutilized or poorly managed. Transforming this waste into biochar could offer a dual opportunity: improving the fertility of arid soils and providing a source of renewable energy. In this study, we focus on the slow pyrolysis of the three types of biomass of varying compositions and origins: millet stalks (TM), which are abundant in Sahelian regions and very often underutilized; cashew nut shells (CA), a by-product of the agri-food industry generated in large quantities; and refrigerated slaughterhouse contents (CP), which are waste products consisting mainly of organic matter. The objective was to evaluate the yields and characteristics of the products resulting from the pyrolysis of these biomasses using a household reactor called a multifunctional household oven (*Tarpilga et al.,2023*), highlighting their energy and agronomic potential as well as their application prospects. Despite extensive research on biomass pyrolysis, most studies are conducted under controlled laboratory conditions using optimized reactors, which often poorly reflect real household applications in developing countries. Moreover, the interaction between biomass properties and low-tech reactor design remains insufficiently documented. This study addresses this gap by investigating the thermochemical behavior and energy efficiency of underexploited local biomasses in a multifunctional household oven, considered as an integrated biomass-reactor system operating under realistic domestic conditions.

2. Materials and Methods

2.1. Pyrolyzer and Gas Detector

The pyrolytic chlorinator used (Figure 1.a) in this study is a cylindrical device. It is also known as a multifunctional household oven. (Tarpilga et al., 2023) It consists of three coaxial compartments: the combustion chamber, the pyrolysis chamber, and the insulation chamber (Figure 1.b). An air duct runs along the central axis of the combustion chamber. The pyrolysis chamber receives the biomass to be pyrolyzed, and the pyrolysis gases are burned in the combustion chamber where they are mixed with air. The insulation chamber limits heat conduction to the outer wall of the furnace. A portable multigas detector (Ex, O_2, CO, H_2S) was used for the semi-quantitative assessment of pyrolysis gases. However, it does not allow for a complete analysis of the syngas composition, which would require gas chromatography (GC) or micro-GC analysis.

 doi:10.20944/preprints202602.1526.v1

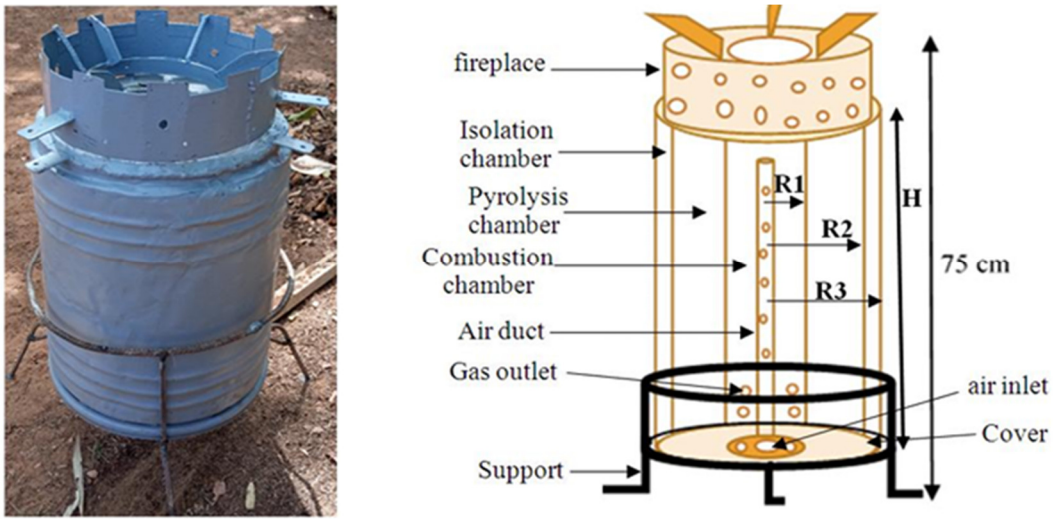

Figure 1. Picture (a) and diagram (b) of the pyrolysis reactor.

2.2. Biomasses

The biomass used consisted of millet stalks, cashew nut shells, and waste from the Bobo-Dioulasso cold storage abattoir. The millet stalks (Figure 2.a) came from a millet field in the village of Legma (11° 13′ 59″ north and 4° 10′ 20″ west), 15 kilometers from the city of Bobo. The cashew nut shells (Figure 2.b) came from *Anatrans*, a local cashew nut shelling factory. There were also pre-treated shells, which are called "cashew nut shell meal" (CSM) (Figure 2.c), collected from an Anatrans annex specializing in the extraction of CNSL (Cashew Nut Shell Liquid). As a reminder, CNSL is a corrosive liquid contained in cashew nut shells. This liquid makes direct combustion of the shells unsuitable because it leads to the formation of highly suffocating and toxic gases. The sludge (Figure 2.d) consists of plant waste from the digestive tract of animals after slaughter. It was collected from the Bobo-Dioulasso refrigerated slaughterhouse located in sector 12 of the said city.

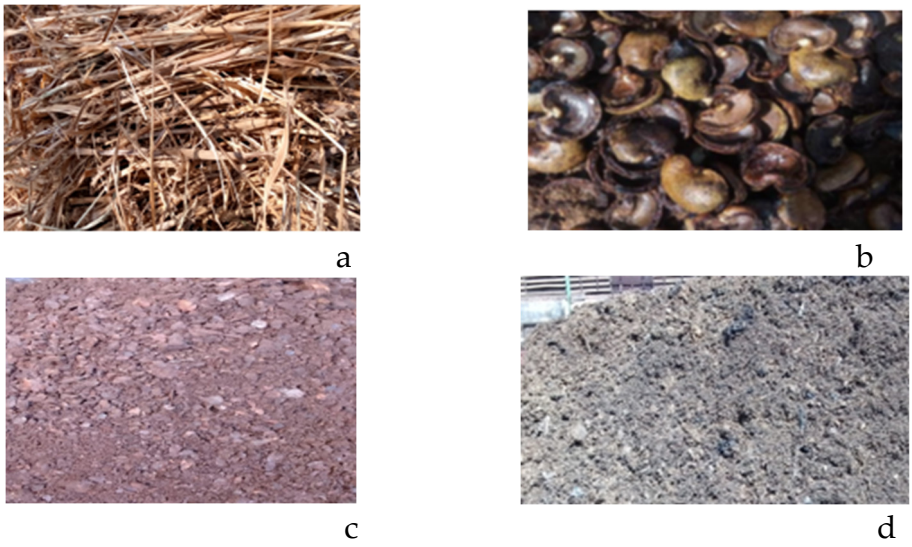

Figure 2. (a)Millet stalks, (b)cashew nut shells, (c)cashew nut cake and (d) contents of pansies.

2.3. Thermocouples and Data Logger

Temperatures were measured using type "K" thermocouples (Figure 3.a) whose extension cables can withstand temperatures of approximately 1000 °C with a standard error of 2.2%. As a reminder, a thermocouple is a sensor that primarily uses the Seebeck effect to obtain a temperature measurement. (Ottello, 19 juin 2021). A 16-input Data Logger (model MS6D) (Figure 3.b), a Lenovo

 doi:10.20944/preprints202602.1526.v1

Core i7 computer, and a connecting cable linking the Data Logger to the computer were required for the measurements. (Tarpilga et al., 2023).

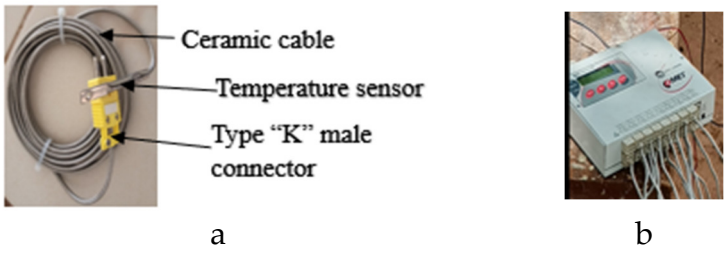

Figure 3. (a)Type 'K' thermocouple and (b) data logger.

3. Methods

The experimental measurements concerned the pyrolysis temperature, the combustion temperatures, and the mass-energy balance.

3.1. Oven Operation

The operation of this pyrolyzer involves several steps (Figure 4). The first step in starting it up is to load the biomass into the pyrolysis chamber. This consists of introducing the biomass into the pyrolysis chamber and closing the lid. The second step is to load the combustion chamber with a solid, dry fuel. This fuel can be wood, corn cobs, or any other biomass with particles measuring 10 cm or larger, and whose combustion does not produce a lot of ash or highly toxic fumes. The final step is to initiate the combustion of the fuel. The heat produced by this combustion is transferred to the biomass in the pyrolysis chamber, which in turn releases gases that are then transferred to the combustion chamber to be burned. Its operation is a closed loop.

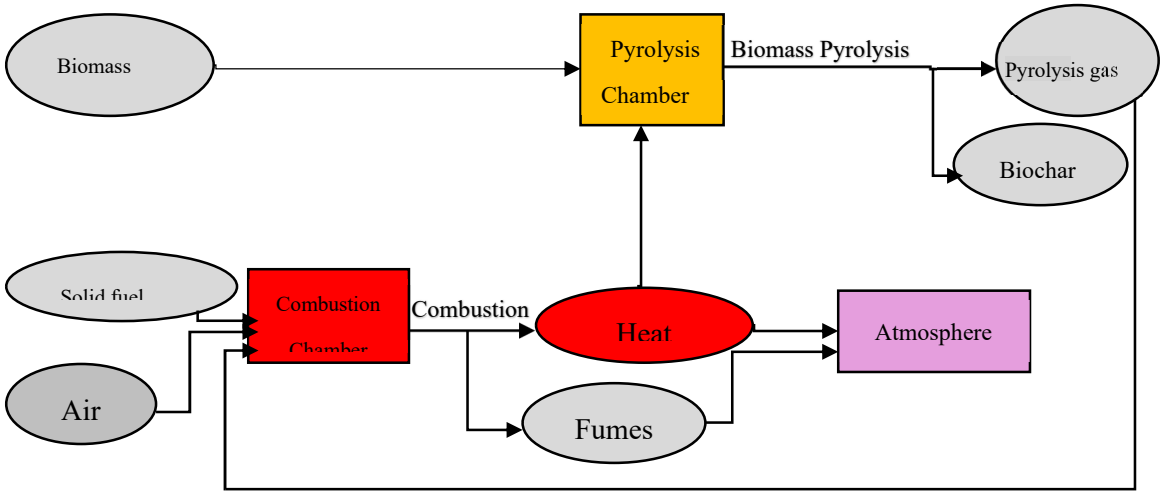

Figure 4. Operation of the pyrolysis reactor.

3.2. Experimental Setup

Figure 5 shows the experimental setup, including the different positions of the thermocouples (Tarpilga et al., 2023). To obtain the temperature data, five thermocouples were first placed in the upper part of the oven: one in the Combustion Chamber (CC), one on the inner wall (PI), one in the Pyrolysis Chamber (CP), one on the outer wall (Pext), and one on the wall in contact with the ambient air (PA). These same thermocouple locations were also used in the middle (along the height) and in the lower part of the oven. Next, the fifteen thermocouples were connected to fifteen inputs of the

 doi:10.20944/preprints202602.1526.v1

Data Logger (which recorded the data), which was itself connected to the computer. Finally, the software called "Ms+Ink" was installed to retrieve the temperature measurements in degrees Celsius. Excel 2016 was used to calculate the average temperatures, and Origin Pro 2020 was used to plot the temperature profiles. The data logger was programmed to measure the temperature every second.

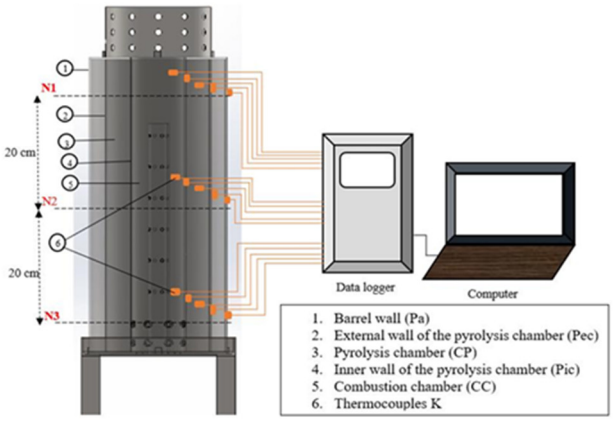

Figure 5. Diagram of the experimental pyrolysis setup.

3.3. Mass-Energy Balance and Performance Indicators

This section describes the calculation methods used to evaluate the performance of the pyrolysis reactor, focusing on the energy efficiency of the process and a systematic comparison of the four biomasses tested. The approach combines a simple mass balance with a first-principles energy balance, allowing the calculation of key performance and efficiency indicators.

3.3.1. Mass and Energy Balance

The masses of introduced biomass (m_{bm}) and produced biochar (m_{char}) were measured directly. The mass of pyrolytic oil (m_{oil}) was collected and weighed. The mass of pyrolytic gases (condensable and non-condensable), m_g, was deduced by conservation of mass according to equation (1). This balance is fundamental for calculating all mass yields.

$$m_g = m_{bm} - [m_{char} + m_{oil}] \quad (1)$$

The total estimated energy Q_{bm} (Kj) of the biomass introduced into the pyrolysis chamber of the furnace is given by equation (2)

$$Q_{bm} = m_{bm} \times PCI_{bm} \quad (2)$$

The quantity of heat Q_g supplied by the combustion of pyrolysis gases is given by equation (3)

$$Q_g = m_{bm} \times PCI_{bm} - [m_{char} \times PCI_{char} + m_{oil} \times PCI_{oil}] \quad (3)$$

This energy could have a complex interpretation because the system functions like a snowball effect. However, we denote Q_{net} as the useful energy supplied to the external environment by the biomass-reactor system and its expression is given by equation (4)

$$Q_{net} = Q_g - \left[m_{char} \times c_{p,char}(T_{char} - T_r) + m_{oil} \times c_{p,oil}(T_{oil} - T_r) + P_{ert.th}\right] \quad (4)$$

where $p_{ert.th}$ refers to losses related to heat transfers through the oven walls and c_p is the specific heat of the biochar or oil produced. The terms $m_{char} \times c_{p,char}(T_{char} - T_r)$ and $c_{p,oil}(T_{oil} - T_r)$ represent the specific sensible energies of biochar and oils, respectively. This energy results from the combustion of gases. In this first-order energy assessment, heat losses through the reactor walls and sensible energy of the products (biochars and oils) were neglected. Although these terms contribute to the overall energy balance, their omission does not affect the comparative analysis between the different biomasses, as their relative values are similar from one sample to another. This simplification allows us to focus on the main energy contributions: the energy released by the combustion of pyrolysis gases. Also, the existence of an isolation chamber in the reactor considerably limits heat losses through the walls, which makes $P_{ert.th}$ very negligible compared to the useful energy of the system. Thus we set up equation 5

 doi:10.20944/preprints202602.1526.v1

$$Q_{net} = Q_g \ (5)$$

For the energy calculations relating to pyrolysis oil from cashew nut shells, a lower heating value (LHV) of 21.7 MJ/kg was used, corresponding to a representative value found in the literature for bio-oil produced from cashew nut shells under mild pyrolysis conditions (~250 °C), which allows to make estimates consistent with the small-scale processes studied (Amaliyah & Putra, 2021).

3.3.2. Performance Indicators

The yield r_{f_i} of pyrolysis in a fraction f_i (biochar, liquid, gas) was evaluated for each of the biomasses used in this study. The yield r_f is given by equation (6)

$$r_{f_i} = \frac{m_{f_i}}{m_{bm}} \times 100 \ (6)$$

Energy efficiency η is the ratio between useful energy and the total energy of the biomass. It is given by equation (7)

$$\eta_{net} = \frac{Q_{net}}{Q_{bm}} \ (7)$$

The heating rate Vcf and the residence time of the biomass in the pyrolysis chamber are also important parameters in biochar production. In this study, we do not control them, but we can calculate them. The residence time corresponds to the end of pyrolysis, and the heating rate is given by equation (8).

$Vcf = 60\left(\frac{\sum_1^N T_{t_{i+1}} - T_{t_i}}{N}\right)$ (8) , $\Delta Vcf = 60.\frac{\sigma_T\sqrt{2}}{N}$

T_{t_i} is the temperature at a time t_i in the pyrolysis chamber, $T_{t_{i+1}}$ is the temperature at a given time t_{i+1} in the pyrolysis chamber, N is the number of measured temperature data points et ΔVcf the error in the heating speed in $°C/min$

4. Results

4.1. Pyrolysis Gas

The main gaseous constituents produced during the pyrolysis of different biomasses in the pyrolysis chamber are presented in Table 1 below. The gases analyzed are residual oxygen (O_2), hydrogen sulfide (H_2S), carbon monoxide (CO) and total hydrocarbons (HC). Carbon monoxide has an average concentration of 1000 ppm for all biomass samples. Oxygen (O_2) levels range from 6.08 ± 1.6 to $11.2 \pm 2.3\%$, H_2S levels from 7.9 ± 3.4 to $85.66 \pm 13.4\ ppm$, and hydrocarbon (HC) levels from 66 ± 18.9 to 100%. The highest O_2 and HC values are observed for gut contents, while cashew nut shells show the highest H_2S content.

Table 1. Composition of pyrolysis gases.

Biomass	Constituents of the gases in the pyrolysis chamber			
	O_2(%Vol)	H_2S (ppm)	CO(ppm)	HC(%LEL)
Millet stalks (TM)	6.6 ± 0.4	7.9 ± 3.4	1000 ± 0	85.8 ± 15.2
Cashew shells (CA)	6.08 ± 1.6	85.66 ± 13.4	1000 ± 0	100
Cashew nut cakes (TCA)	6.1 ± 2	76 ± 23	1000 ± 0	100
Gut contents (CP)	11.2 ± 2.3	8.83 ± 3.8	1000 ± 0	66 ± 18.9

ppm: parts per million, **LEL**: Lower Explosive Limit.

4.2. Temperature Profile

Appendix A provides the temperature profiles measured in the different compartments and walls of the furnace for each of the biomasses studied. Figures 6 and 7 respectively represent the temperature profiles in the pyrolysis chamber (PC) and the combustion chamber (CC) of the reactor, obtained during the pyrolysis of four biomasses: cashew shells (CA), cashew shell meal (TCA),

 doi:10.20944/preprints202602.1526.v1

Rumen contents (PC) and millet stalks (TM). The temperature curves show generally similar patterns for both chambers and the four biomasses. They successively exhibit an initial phase where temperatures evolve in tandem, a distinct growth phase for each biomass, a stabilization phase, the duration of which varies depending on the biomass and the reactor compartment, and a final decay phase. Analysis of the combustion chamber profile (Figure 7) reveals maximum temperatures of approximately 650 °C for cashew shells, 680 °C for cashew shell meal, 700 °C for the contents of the seeds, and 800 °C for millet stalks. For the pyrolysis chamber (Figure 6), the maximum temperatures reached are approximately 350 °C for millet stalks, 310 °C for cashew shells, 295 °C for cashew shell meal, and 270 °C for the contents of the seeds.

The residence times in this study correspond to the time elapsed between the start and end of pyrolysis in the pyrolysis chamber. The residence times were 4 hours, 2 hours 40 minutes, 2 hours, and 1 hour 10 minutes for cashew nut cake, cashew nut shells, and millet stalks, respectively.

The heating rate during pyrolysis was $5.42 \pm 0.05°C/min$, $3.42 \pm 0.03°C/min$, $2.07 \pm 0.02°C/min$, and $1.22 \pm 0.01°C/min$ for millet stalks, rumen contents, cashew nut shell, and cashew nut shell cake, respectively (Figure 8).

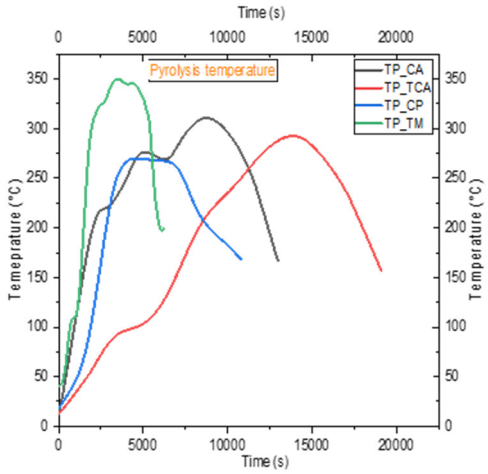

Figure 6. Pyrolysis temperature of biomass.

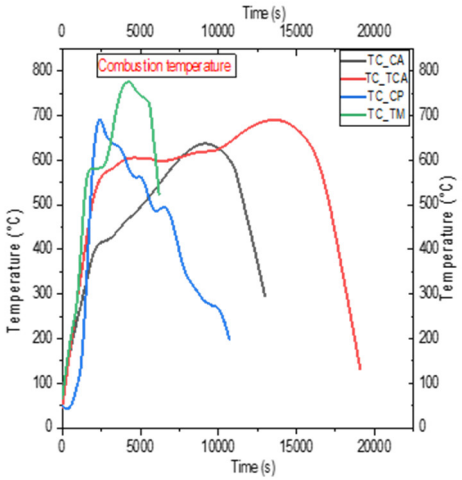

Figure 7. Combustion temperature of biomass.

 doi:10.20944/preprints202602.1526.v1

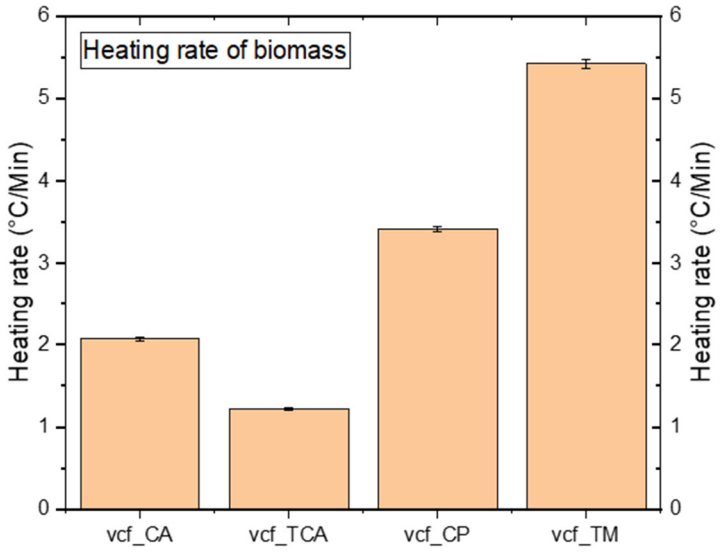

Figure 8. Heating rate of millet stalks ™, rumen contents (CP), cashew nut shell (CA), and cashew nut shell cake (TCA).

4.3. Pyrolysis efficiency

The yields of biochar (solid), liquid and gas during the thermochemical degradation of the different biomasses studied are compared with each other. The yields obtained were compared (Figure 9). The values of these yields, respectively for solids, gases, and liquids, were $30.52 \pm 0.35\%$, $52.96 \pm 0.47\%$, and $16.5 \pm 0.11\%$ for cashew nut shells; $54.67 \pm 2.88\%$, $45.33 \pm 2.88\%$, and $0.0 \pm 0.0\%$ for cashew nut shell cake; $58.54 \pm 1.22\%$, $41.46 \pm 1.22\%$, and $0.0 \pm 0.0\%$ for gut contents; and $43.06 \pm 2.83\%$, $56.93 \pm 2.83\%$, and $0.0 \pm 0.0\%$ for millet stalks. The reactor's energy efficiency was highest with cashew nut shells (70.59%), followed by millet stalks (70.54%) cashew nut shell meal (46.35%) and finally intestinal contents (39.66%).

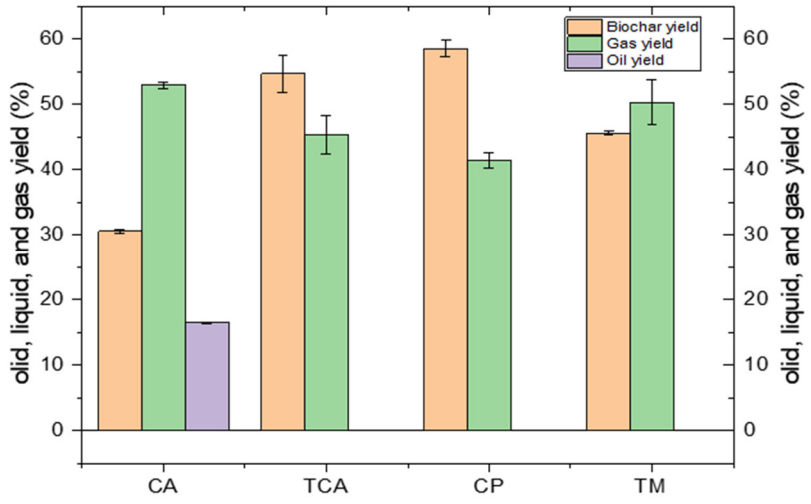

 doi:10.20944/preprints202602.1526.v1

Figure 9. Pyrolysis yeld of millet stalks (TM), cashew nut shell (CA), cashew nut shell cake (TCA) and rumen contents (CP) throught the pyrolysis reactor.

5. Discusssion

5.1. Pyrolysis Gas

The gaseous composition resulting from pyrolysis showed a predominance of carbon monoxide (CO), confirming the results of (Li et al., 2024) who attributed this high proportion to the breaking of C-O and C=O bonds during thermal decomposition. However, it should also be noted that under the conditions of this work, fumes from the combustion chamber could pass into the pyrolysis chamber and significantly alter these CO proportions. The differences observed in residual oxygen (O_2) levels reflect varying degrees of conversion, as also pointed out by Moreira *et al*. (2017) by linking the gaseous composition to the devolatilization rate. The high hydrogen sulfide (H_2S) emissions from cashew nut shells and meal confirmed the conclusions of Das et Ganesh (2004), these findings indicated that biomass rich in nitrogen and sulfur compounds releases more sulfur gases. Furthermore, the high total hydrocarbon (HC) levels in cashew rumen and meal contents appear to be mitigated because these two biomasses have very different volatile content levels. This supports the idea that the two chambers could exchange gases. Nevertheless, these values are important for understanding the energy potential of these gases within the pyrolysis chamber.

5.2. Analysis of Temperature Profiles

The temperature profiles recorded during the various pyrolysis experiments show comparable thermal dynamics. These dynamics are characterized by four successive phases: an initial phase of slow and simultaneous temperature increase in the different compartments of the reactor, a phase of differentiated growth depending on the zone, a stabilization phase of varying duration depending on the biomass used, and finally, a phase of gradual decrease. This similarity in the shape of the curves confirms the consistent thermal behavior of the pyrolysis system, regardless of the type of biomass, while highlighting significant differences in the intensity and duration of the phases depending on the biomass used. Indeed, several studies of biomass pyrolysis, such as those by (Lewandowski et al., 2020; El-Sayed et al., 2024), have shown that the thermal profiles follow a series of stages. The first is an initial rise linked to drying, the second an active decomposition corresponding to the release of volatiles, the third, more stable phase of biochar formation, and a final decay phase.

These results confirm a consistent dynamic of the pyrolysis system, regardless of the type of biomass, while highlighting that the intensity and duration of the phases depend on the nature of the material. The observed hierarchy of combustion temperatures results from the interaction between the gasification potential of each biomass and the reactor's efficiency in burning the produced gases. These results suggest that the physicochemical nature of the biomass and the reactor characteristics directly influence its energy capacity and, consequently, the temperature reached in the combustion chamber. As established by (A Demirbas, 2004) and (McKendry, 2002), the millet stalks reached the highest temperatures because their composition produces a pyrolysis gas rich in fuels with high calorific value. However, this potential energy is only fully released through an optimal reactor design. The work of (Nussbaumer, 2003) showed that a well-designed combustion chamber, allowing for efficient air-gas mixing, is essential for completely converting chemical energy into heat.

However, the difference in maximum temperatures observed in the pyrolysis chamber (millet stalks ≈ 350 °C vs. grains ≈ 270 °C) is also explained by physicochemical properties such as thermal conductivity and biomass particle density. Indeed, higher density and compact morphology promote better heat transfer (Wang et al., 2023; Mehrabian et al., 2012), while higher residual humidity lowers the effective temperature by absorbing the energy required for evaporation (Ayhan Demirbas, 2004). Furthermore, the lignocellulosic composition (cellulose, hemicellulose and lignin) modulates the

 doi:10.20944/preprints202602.1526.v1

characteristic decomposition temperatures, explaining the differences observed depending on the type of biomass.

The residence times observed reflect different pyrolysis rates, which appear to be correlated with the density and porosity of the material residing in the pyrolysis chamber. These observations corroborate those of (Luo et al., 2010; Kan et al., 2016),who demonstrated that the density, porosity, and lignocellulosic structure of biomass influence the pyrolysis rate. Compact, low-porosity materials exhibit slower heat diffusion, thus requiring a longer residence time for complete decomposition, unlike lighter, more fibrous biomass. Nevertheless, these durations, which correspond to the reactor's operating time, are more or less sufficient for cooking local Burkinabé foods. The heating rate, on the other hand, is inversely proportional to the residence time: it is highest for millet stalks (5.42 °C/min) and lowest for cashew nut meal (1.22 °C/min), further highlighting the effect of the biomass's structure, composition, and particle size on the thermal dynamics of the process.

The comparative study between raw cashew nut shells and cashew nut meal reveals distinct thermal behavior in the combustion chamber and pyrolysis chamber. Pretreatment of the hulls seems to promote better thermal accessibility, resulting in a more pronounced increase in combustion temperature, but slower pyrolysis, which may be due to the reduction of volatile compounds after oil extraction, thus allowing better control of the pyrolysis gas flow to the combustion chamber.

5.3. Pyrolysis Efficiency

The mass yields observed show a strong correlation between the initial composition of the biomass and the pyrolysis conditions (M. Vilas-Boas et al., 2024). This variation can be explained by the difference in lignocellulosic structure, volatile compound content, and mineral content of the raw materials, which influence thermal decomposition and product distribution.

The difference in the combustion flames of pyrolysis gases (Appendix B) is an important indicator of the impact of the physicochemical properties of biomass on the energy efficiency of the system.

The high gaseous content of the hulls results from the degradation of CNSL and phenolic compounds, which generate large quantities of light gases (CO, CO_2, C_xH_y) and condensable oils, as indicated by (Chung et al., 2024).

Their high content of energy-rich organic compounds also explains the high energy yield (70.59%) observed for cashew nut shells (Amaliyah & Putra, 2021). Conversely, the loss of CNSL reduces the volatile fraction available in the oilseed cake and promotes the formation of a larger carbon residue, dominated by fixed materials and minerals. This corroborates the results obtained by (M. Vilas-Boas et al., 2024), who found that removing the liquid from cashew nut shells (CNSL) during pretreatment decreases the volatile matter content and increases the fixed carbon and ash fractions in the solid residue.

The high solid yields without significant liquid formation in millet stalks and husks suggest either a low content of condensable precursors or operating conditions that promote thermal cracking of tars.

High temperatures and prolonged residence times can accentuate the breaking of carbon chains and transform tars into light gases.(Liu,2018).

The presence of mineral impurities or sand in the gut contents could also explain the high proportion of biochar, as these inert elements artificially increase the apparent solids yield.

The energy results confirm that the simple mass of biochar is not linearly correlated with energy recovery.

Energy is primarily concentrated in the gas and liquid phases, which explains why biomasses producing more gas, such as cashew nut shells, have a better overall energy yield. This observation is consistent with the work described in (« Energy Production from Biomass (Part 1) », 2002), which showed that the distribution of energy between phases depends more on the chemical reactivity of volatile compounds than on total mass yield.

 doi:10.20944/preprints202602.1526.v1

The efficiency of biomass conversion (in biochar, liquid, gas) vary significantly from one biomass to another, highlighting their structural and chemical differences. Cashew nut shells exhibit the typical characteristics of a material rich in volatile compounds, with a dominant gas yield ($52.96 \pm 0.47\%$) a low solids yield ($30.52 \pm 0.35\%$), and an intermediate liquid yield ($16.5 \pm 0.11\%$).

In contrast, cashew nut shell meal, which lacks a large proportion of its free-seed monomers (FSM) (liquid), shows a very high biochar yield ($54.67 \pm 2.88\%$,) and zero liquid yield. This result reflects the low volatile matter content and the predominance of the fixed fraction in the material.

The rumen content and millet stalks also showed a high solids yield ($58.54 \pm 1.22\%$ and $43.06 \pm 2.83\%$, respectively) and no liquid was detected, suggesting that their condensable compound content is very low or that the operating conditions favored their thermal cracking. However, the biochar yield of the rumen content could be influenced by the presence of sand in the raw material due to handling and storage conditions at the site. It should be noted that the visual nature of the biochars produced (Appendix C) reinforces the difference between the thermal processes used, which must be mastered and considered in the design of domestic reactors in order to obtain high-quality biochar.

6. Conclusion

The study of the slow pyrolysis of millet stalks, cashew nut shells, and slaughterhouse waste, conducted using a multi-function home oven, allowed for the characterization of thermal and energy behaviors specific to each biomass under realistic domestic operating conditions. The pyrolysis temperature profiles recorded revealed a succession of typical phases with maximum temperatures ranging from 270 to 350 °C depending on the type of biomass. Millet stalks reached the highest pyrolysis temperatures (≈ 350 °C), associated with a relatively short residence time (≈ 1 h 10 min), while cashew nut shells and their meal required longer residence times (approximately 4 h) due to their density and a high oil content. Slaughterhouse waste, on the other hand, exhibited an intermediate behavior with a progressive thermal degradation and a continuous energy release. The pyrolysis yields obtained clearly reflected these differences: cashew nut shells produced a significant proportion of gas and liquid (overall energy yield ≈ 70%), while millet stalks and slaughterhouse waste generated more biochar, which can be used as a soil amendment. These results confirm that energy is primarily concentrated in the gas and liquid phases, and that biomass that promotes the production of these fractions offers better energy efficiency. However, these results suggest categorizing biomasses according to their volatile components and adapting the reactor parameters to each group to optimize the energy efficiency of the reactor-biomass system. The multifunctional family oven has thus proven suitable for the integrated valorization of local biomass, combining energy (gas) and biochar production with agronomic potential. This device represents an accessible, sustainable, and replicable solution for decentralized energy transition in rural areas of Africa and the Sahel in particular. Work is currently underway to analyze the combustion fumes from pyrolysis gases and characterize the biochar produced in order to take into account user health and evaluate the agronomic potential of the biochar.

Acknowledges: This work was supported by the European Union Commission through the AFRIDI project, which aims to strengthen higher education and research in Africa.

Conflicts of Interest: The authors declare no conflicts of interest.

Appendix A

Temperature profile in the different compartments and walls of the pyrolysis reactor during the pyrolysis of cashew hulls (CA), cashew hull meal (TCA), millet stalks (TM) and rumen contents (CP)

 doi:10.20944/preprints202602.1526.v1

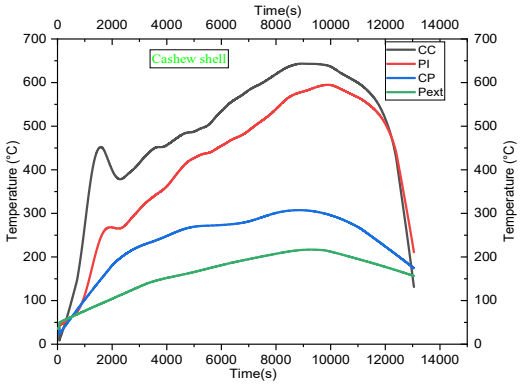

Figure A1. Cashew Shell temperature profile.

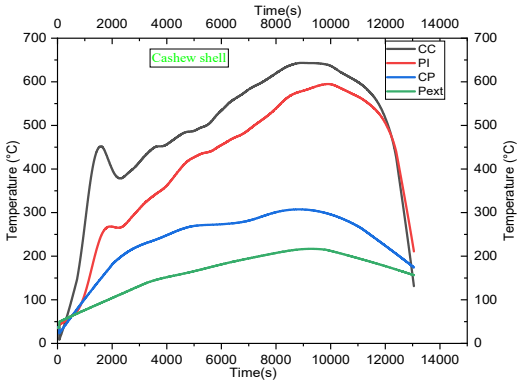

Figure A2. Cashew Shell meat temperature profile.

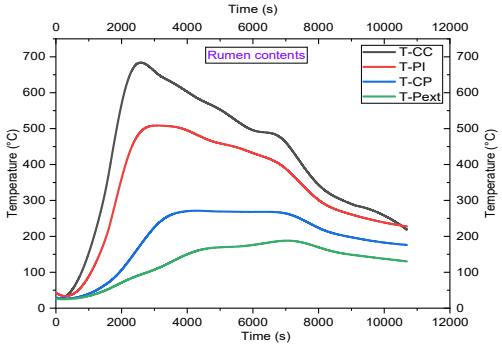

Figure A3. Rumen contents temperature profile.

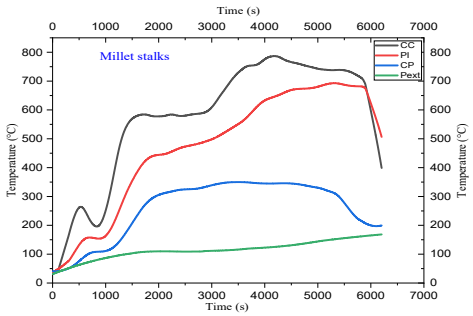

Figure A4. Millet stalks temperature profile.

 doi:10.20944/preprints202602.1526.v1

Appendix B

Comparison of combustion flames of pyrolysis gases of millet stems (TM), cashew hulls (CA), cashew hull cakes (TCA) and rumen contents.

The intensity of the combustion flames from pyrolysis gases varied significantly depending on the type of biomass used. Observation of the flames (Figure B) revealed that cashew nut shells produced the largest flames (Figure B4), followed by cashew nut shell cake (Figure B3), gut contents (Figure B2), and finally millet stalks (Figure B1), which generated the smallest flames. Furthermore, a notable difference in color was observed. Shells and cakes produced yellow flames. Millet stalks and gut contents generated orange flames, which are almost invisible at the reactor nozzle. Their stability also differed. At this point, the flames from the shells and meal, although initially unstable, subsequently stabilized. This stabilization phenomenon was not observed with millet stalks and gut contents. Finally, regarding emissions, no white fumes were observed for any of the biomasses tested. However, it was particularly noteworthy that for cashew nut shells and cakes, the suffocating nature of the fumes emanating from direct combustion was completely absent during pyrolysis.

Figure 1. millet stalks, (2) contents of grains, (3) cashew nutshell cake and (4) cashew shells.

Appendix C

The biochars of millet stems (Figure C1), cashew shells (Figure C2), cashew shell meal (Figure C3), and rumen contents produced during the pyrolysis of the study biomasses using the multifunctional family oven

Figure 1. millet stalks, (2) cashew shells, (3) cashew shell meal and (4) gut contents.

References

1. Amaliyah, N., & Putra, A. E. E. (2021). Microwave-Assisted Pyrolysis of Cashew Nut Shell. International Journal of Design & Nature and Ecodynamics, 16(2), 227--232. https://doi.org/10.18280/ijdne.160213
2. Armah, E. K., Chetty, M., Adedeji, J. A., Estrice, D. E., Mutsvene, B., Singh, N., Tshemese, Z., Armah, E. K., Chetty, M., Adedeji, J. A., Estrice, D. E., Mutsvene, B., Singh, N., & Tshemese, Z. (2022). Biochar: Production, Application and the Future. In Biochar—Productive Technologies, Properties and Applications. IntechOpen. https://doi.org/10.5772/intechopen.105070

 doi:10.20944/preprints202602.1526.v1

3. C.F.D.T, & agro-alimentaire, F. générale. (1981). Alternative pour aujourd'hui: La biomasse, énergie verte. FeniXX.
4. Chormare, R., Moradeeya, P. G., Sahoo, T. P., Seenuvasan, M., Baskar, G., Saravaia, H. T., & Kumar, M. A. (2023). Conversion of solid wastes and natural biomass for deciphering the valorization of biochar in pollution abatement: A review on the thermo-chemical processes. Chemosphere, 339, 139760. https://doi.org/10.1016/j.chemosphere.2023.139760
5. Chung, K. W. Y., Blin, J., Lanvin, C., Martin, E., Valette, J., & Van De Steene, L. (2024). Pyrolysis of cashew nut shells-focus on extractives. Journal of Analytical and Applied Pyrolysis, 179, 106452. https://doi.org/10.1016/j.jaap.2024.106452
6. Demirbas, A. (2004). Combustion characteristics of different biomass fuels. Progress in Energy and Combustion Science, 30(2), 219--230. https://doi.org/10.1016/j.pecs.2003.10.004
7. Demirbas, Ayhan. (2004). Effect of initial moisture content on the yields of oily products from pyrolysis of biomass. Journal of Analytical and Applied Pyrolysis, 71(2), 803--815. https://doi.org/10.1016/j.jaap.2003.10.008
8. El-Sayed, S. A., Khass, T. M., & Mostafa, M. E. (2024). Thermal degradation behaviour and chemical kinetic characteristics of biomass pyrolysis using TG/DTG/DTA techniques. Biomass Conversion and Biorefinery, 14(15), 17779--17803. https://doi.org/10.1007/s13399-023-03926-2
9. Energy production from biomass (part 1): Overview of biomass. (2002). Bioresource Technology, 83(1), 37--46. https://doi.org/10.1016/S0960-8524(01)00118-3
10. Graça, J., Kwapinska, M., Murphy, B., Duggan, T., Leahy, J. J., & Kelleher, B. (2024). Pyrolysis, a recovery solution to reduce landfilling of residual organic waste generated from mixed municipal waste. Environmental Science and Pollution Research, 31(21), 30676--30687. https://doi.org/10.1007/s11356-024-33282-1
11. Kan, T., Strezov, V., & Evans, T. J. (2016). Lignocellulosic biomass pyrolysis: A review of product properties and effects of pyrolysis parameters. Renewable and Sustainable Energy Reviews, 57, 1126--1140. https://doi.org/10.1016/j.rser.2015.12.185
12. Laurent, P., Roiz, J., Wertz, J.-L., Richel, A., & Paquot, M. (2011). Le bioraffinage, une alternative prometteuse à la pétrochimie. BASE. https://popups.uliege.be/1780-4507/index.php?id=8007
13. Lewandowski, W. M., Ryms, M., & Kosakowski, W. (2020). Thermal Biomass Conversion: A Review. Processes, 8(5), 516. https://doi.org/10.3390/pr8050516
14. Li, J., Lin, L., Ju, T., Meng, F., Han, S., Chen, K., & Jiang, J. (2024). Microwave-assisted pyrolysis of solid waste for production of high-value liquid oil, syngas, and carbon solids: A review. Renewable and Sustainable Energy Reviews, 189, 113979. https://doi.org/10.1016/j.rser.2023.113979
15. Liu, Q. D. Z. C. F. H. Y. Z. J. Y. S. G. H. (2018). Influences of Temperature and Residence Time on Secondary Reactions of Volatiles from Coal Pyrolysis. The Chinese Journal of Process Engineering, 18(1), 140. https://doi.org/10.12034/j.issn.1009-606X.217192
16. Luo, S., Xiao, B., Hu, Z., & Liu, S. (2010). Effect of particle size on pyrolysis of single-component municipal solid waste in fixed bed reactor. International Journal of Hydrogen Energy, 35(1), 93--97. https://doi.org/10.1016/j.ijhydene.2009.10.048
17. McKendry, P. (2002). Energy production from biomass (part 1): Overview of biomass. Bioresource Technology, Reviews Issue, 83(1), 37--46. https://doi.org/10.1016/S0960-8524(01)00118-3
18. Mehrabian, R., Scharler, R., & Obernberger, I. (2012). Effects of pyrolysis conditions on the heating rate in biomass particles and applicability of TGA kinetic parameters in particle thermal conversion modelling. Fuel, 93, 567--575. https://doi.org/10.1016/j.fuel.2011.09.054
19. M. Vilas-Boas, A. C., C. Tarelho, L. A., M. Oliveira, H. S., S. Silva, F. G. C., T. Pio, D., & A. Matos, M. A. (2024). Valorisation of residual biomass by pyrolysis: Influence of process conditions on products. Sustainable Energy & Fuels, 8(2), 379--396. https://doi.org/10.1039/D3SE01216F
20. Nussbaumer, T. (2003). Combustion and Co-combustion of Biomass: Fundamentals, Technologies, and Primary Measures for Emission Reduction. Energy & Fuels, 17(6), 1510--1521. https://doi.org/10.1021/ef030031q

 doi:10.20944/preprints202602.1526.v1

21. Paudel, P. P., Kafle, S., Park, S., Kim, S. J., Cho, L., & Kim, D. H. (2024). Advancements in sustainable thermochemical conversion of agricultural crop residues: A systematic review of technical progress, applications, perspectives, and challenges. Renewable and Sustainable Energy Reviews, 202, 114723. https://doi.org/10.1016/j.rser.2024.114723
22. Siddiqui, M. T. H., Nizamuddin, S., Mubarak, N. M., Shirin, K., Aijaz, M., Hussain, M., & Baloch, H. A. (2019). Characterization and Process Optimization of Biochar Produced Using Novel Biomass, Waste Pomegranate Peel: A Response Surface Methodology Approach. Waste and Biomass Valorization, 10(3), 521--532. https://doi.org/10.1007/s12649-017-0091-y
23. Tarpilga et al.,2023. (s. d.). Consulté 8 mai 2025, à l'adresse https://www.elixirpublishers.com/articles/1682592793_202303002.pdf
24. Tarpilga, M., Ouedraogo, F., Gounkaou, Y., Da, F., Ouedraogo, S., & Naon, B. (2023). Temporal Temperature Evolusion during the Pyrolisis of Cotton Stalks, Corn Stalk and Rice Husk Using Multifunction Family Oven for the Biochar Production. International Journal of Plant & Soil Science, 35, 336--347. https://doi.org/10.9734/ijpss/2023/v35i193560
25. Wang, P., Yu, J., Liu, X., & Millan, M. (2023). On the effect of pellet density on biomass pyrolysis in a pressurized fixed bed reactor. Fuel, 354, 129191. https://doi.org/10.1016/j.fuel.2023.129191